Check for updates

Research progress on adsorption and separation of carbonyl sulfide in blast furnace gas

Ying Wang, [ID] Xiaoqin Wu,* Di Wei, Yue Chen, Jia Yang and LvYou Wu

The iron and steel industry is one of the foundational industries in China. However, with the introduction of energy-saving and emission reduction policies, desulfurization of blast furnace gas (BFG) is also necessary for further sulfur control in the iron and steel industry. Carbonyl sulfide (COS) has become a significant and difficult issue in the BFG treatment due to its unique physical and chemical properties. The sources of COS in BFG are reviewed, and the commonly used removal methods for COS are summarized, including the types of adsorbents commonly used in adsorption methods and the adsorption mechanism of COS. The adsorption method is simple in operation, economical, and rich in types of adsorbents and has become a major focus of current research. At the same time, commonly used adsorbent materials such as activated carbon, molecular sieves, metal–organic frameworks (MOFs), and layered hydroxide adsorbents (LDHs) are introduced. The three mechanisms of adsorption including π-complexation, acid–base interaction, and metal–sulfur interaction provide useful information for the subsequent development of BFG desulfurization technology.

Key Laboratory of Hubei Province for Coal Conversion and New Carbon Materials, School of Chemistry and Chemical Engineering, Wuhan University of Science and Technology, China. E-mail: wuxiaoqin@wust.edu.cn

Ying Wang: (1997), born in Baoji City, Shaanxi Province, is a third-year graduate student of Wuhan University of Science and Technology and is mainly engaged in studies related to the removal of carbonyl sulfur from blast furnace gas and the preparation and modification of related adsorbents.

Xiaoqin Wu: (1972), born in Wuhan, Hubei, is professor and director of the Teaching and Research Department of Chemical Technology, Wuhan University of Science and Technology, expert database of Hubei Science and Technology Department. She has conducted related research on the treatment of gaseous pollutants, bioenhancement technology of wastewater treatment, and treatment of industrial solid wastes. She participated in and took charge of the related sub-projects of the "Tenth Five-Year Plan" and "Eleventh Five-Year Plan" 863 Plan of the Ministry of Science and Technology successively, carried out related research on the flue gas desulfurization process of power plants, and participated in the development of characteristic activated carbon and related research on the treatment of heavy metals by the National Natural Science Foundation as the main researcher. The research directions are: (1) research on the utilization of industrial solid waste, (2) air and water pollution control technology, (3) separation and purification technology, (4) new energy development, (5) environmental chemical industry, (6) air pollution control, (7) water pollution control, (8) industrial solid waste recycling, and (9) systems engineering.

The iron and steel industry is an important part of Chinese economy. The output of iron and steel has been ranked first in the world for 24 consecutive years, which reached up to 877 million tons in 2021.[1,2] As a traditional basic industry, large amounts of materials and energy are used in the production process, and there are many engineering and environmental problems that need to be solved urgently. One of the problems is the emission control of gas pollutants such as sulfur oxides and nitrogen oxides.[3,4] Therefore, it is necessary to implement ultra-low emission policy in the iron and steel industry for further achieving environmental protection goals and serving ecological civilization strategies.[5,6]

Iron and steel enterprises are not only consumers of materials and energy but also producers of secondary energy, such as coke oven gas (COG), blast furnace gas (BFG) and converter gas (LDG), which are also important energy sources and raw materials. The green and efficient utilization of these gases is of great significance to the "two-carbon" goal and environmental protection. In recent years, the application of BFG combustion has become a new point of SO_2 emission reduction. Analysis shows that it is mainly derived from the organic sulfur components in BFG. Therefore, in order to effectively control SO_2 emission from BFG, source reduction of sulfur in BFG is imperative.

1 BFG desulfurization application and research trends

The main sulfur-containing compound in BFG is organic sulfur, accounting for more than 80% of the sulfur-containing components.[7–9] The main components are carbonyl sulfide (COS), carbon disulfide (CS_2), thiophene sulfur, *etc.* Some of the physicochemical properties of COS are shown in Table 1, and Fig. 1 is the schematic of the molecular structure of COS. COS is weak in acidity, small in polarity, and difficult to be separated. Limited by technical conditions and economic costs, COS has become a difficult point in BFG desulfurization.

Presently, the technical routes of removing COS can be divided into two categories: one is the wet method and the other is the dry method. The wet method is relatively mature in industrial applications. Generally, liquids such as aqueous solutions or lye solutions (MDEA method, MSQ method, *etc.*) are used to absorb sulfur-containing gases.[10,11] COS is converted into elemental sulfur for recycling. However, there are problems such as easy corrosion of equipment, difficult waste liquid treatment, and high operating costs in the wet method. Typical dry methods include hydrogenation reduction method, hydrolysis method, and adsorption method,[12,13] which have the advantages of strong applicability, no corrosion, and simple operation but high technical requirements for operation, which

Di Wei: (1998), born in Wuhan, Hubei Province, is a third-year graduate student of Wuhan University of Science and Technology and is mainly engaged in studies involving the removal of carbonyl sulfur from blast furnace gas and the preparation and modification of related adsorbents.

Jia Yang: (1997), born in Hanchuan City, Hubei Province, the second-year postgraduate of Wuhan University of Science and Technology, mainly engaged in the removal of carbonyl sulfur from blast furnace gas and the preparation and modification of related adsorbents.

Yue Chen: (1998), born in Fuyang City, Anhui Province, the second-year postgraduate of Wuhan University of Science and Technology, mainly engaged in the removal of carbonyl sulfur from blast furnace gas and the preparation and modification of related adsorbents.

LvYou Wu: (2000), born in Liling, Hunan Province, the second-year postgraduate of Wuhan University of Science and Technology, mainly engaged in the removal of carbonyl sulfur from blast furnace gas and the preparation and modification of related adsorbents.

Table 1 Physical properties of COS

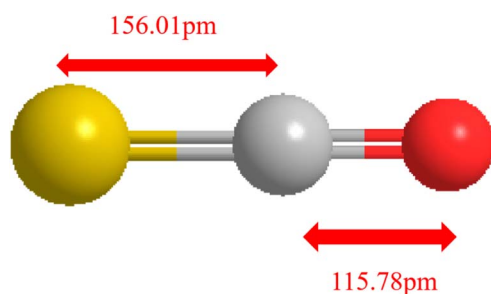| Project	COS
Relative molecular mass	60.07
Melting point (°C)	−138.2
Boiling point (°C)	−50.2
Molecular structure	Straight
Bond length (pm)	116 (C–O); 156 (C–S)
Bond angle (°)	180
Key energy (kJ mol^{-1})	299.5 (OC–S); 593.3 (O–CS)
Dipole moment (D)	0.72

156.01pm

115.78pm

Fig. 1 Chemical structure of carbonyl sulfide.

limits the widespread promotion in the market. With the development of adsorption method, researchers have found that trace amounts of sulfur can deactivate the adsorbent and affect the desulfurization performance.[12,14–16] Experimental results had proved that 4.00 mg of sulfur could reduce the activity of 1.00 g adsorbent Fe–Cu–K by about half.[5,6,17,18] The crucial parameters for the adsorbent are selectivity, sulfur capacity, desulfurization strength, and stability, and further depth research on the performance indicators of comprehensive consumption should be carried out.

1.1 Absorption method

Absorption methods are commonly used in industries for large-scale industrial gas separation such as the separation of carbon dioxide (CO_2) and hydrogen sulfide (H_2S).[19] It is also adequate to organic sulfur removal, and chemical absorption is more effective than physical absorption. Organic amine solutions such as monoethanolamide (MEA), diethanolamine (DEA), diethylene glycol amine (DGA), diisopropanolamine (DIPA), and methyl diethanolamine (MDEA) are usually selected as COS absorbents. Table 2 shows the kinetic study of COS reaction

system with common absorbent solution. They can react with COS to generate corresponding thiamine salts for separation purposes, such as the alkyl alcohol amine method.[20] A zwitterion mechanism could be used to describe the reaction of COS with primary amines (denoted here as AmH), which was similar to the absorption of carbon dioxide:[21]

$$COS + AmH \rightarrow AmH + COS^- \tag{1}$$

$$AmH + COS^- + B \rightarrow AmCOS^- + BH^+ \tag{2}$$
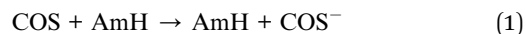
Rivera-Tinoco et al.[25] studied the absorption of COS by dissolving DEA in methanol and modeled the process by a two-step method based on the zwitterion mechanism. However, in the process of alkanolamine desulfurization, part of the solvent will evaporate, the cost of the method is high, and by-products are easily produced, which will have impact on the environment.[26,27] Second, the absorption method cannot reduce total sulfur (mass fraction) to less than 10^{-6} and is not suitable for the fine removal of COS. Therefore, it is necessary to develop catalysts with stable desulfurization performance to reduce process pollution and equipment loss, and improve the precision of COS drop rate.

1.2 Hydrolysis method

The hydrolysis method was originally used to remove H_2S in the Claus process tail gas,[28] and later it was gradually applied in the fields of industrial gas desulfurization and industrial tail gas treatment. The process mechanism is that COS reacts with H_2O to generate H_2S and CO_2:

$$COS + H_2O \rightarrow H_2S + CO_2 \tag{3}$$
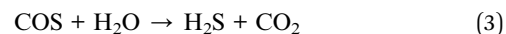
The applicable temperature of the reaction is from 30 to 250 °C, and low temperature appears better for the reaction. Most of the hydrolysis catalysts play their role depending deeply on supports. The two common supports are metal oxides, such as γ-Al_2O_3, and non-metallic oxidants, such as activated carbon.[29,30] Wang et al.[31] explored the separation reaction of COS on Al_2O_3, and found that COS would preferentially undergo hydrolysis with water vapor and then undergo an oxidation reaction on an Al_2O_3 support. David et al.[32] explored the reaction of COS and hydrogen cyanide (HCN) on titanium dioxide (TiO_2) and found that there is a certain degree of competitive adsorption between the reaction sites of the two components. On this basis, by adjusting the pore size of the catalyst, it was

Table 2 Kinetic study of COS-aqueous reaction system

Absorbent	Temperature/K	Solution/kmol m^{-3}	Assumed rate constant/s^{-1}	Quadratic rate constant/m^3 kmol^{-1} s^{-1}	References
MEA	298	1	16		21
MEA	298	1	15.1		22
DGA	300	5.7		2.3	23
DEA	298	1	11		21
MDEA	298	1.26–2.6		0.9	24

Table 3 Hydrolysis of COS on different catalysts

Catalyst	Modification method	Active site	References
2D-NHPC[a]	Nitrogen doping	Pyrrole nitrogen	34
HTLCs[b]	Adjusting the Al/Ce ratio	–OH	35
Fe/MCSAC[c]	NH_3	$-NH_2$	36
NPC[d]	Nitrogen doping	Pyridine/pyrrole nitrogen	37
CuO/Fe_2O_3	Metal oxide	O–S/Fe–C	38
Mg/Al/Ce composite oxide	Metal oxide	M–OH	39
Graphene	Import C	Parallel graphene C–C sites	40
Cu–Fe/TSAC[e]	Metal oxide, O_2	CuO, O_2	41
$Fe_2O_3/AC[f]$	Metal oxide	Fe_2O_3	42

[a] 2D-NHPC: carbonization of urea and glucose to synthesize graphitized two-dimensional micro–meso–macroporous carbon [b] HTLCs: Mg/Al/Ce-like hydrotalcite-like compounds. [c] Fe/MCSAC: Fe-iron-based microwave coconut shell activated carbon. [d] NPC: nitrogen-doped porous carbon. [e] Cu–Fe/TSAC: preparation of Tobacco Stem Activated Carbon (TSAC) catalysts containing copper oxide and Fe_2O_3 by sol–gel method. [f] Fe_2O_3/AC: activated carbon loaded with Fe_2O_3.

found that the desulfurization performance can be effectively improved by increasing the specific surface area and surface basicity of the catalyst. Liang et al.[33] synthesized ordered mesoporous carbons with basic sites by self-assembly, which could completely convert COS into H_2S, and the abundant basic sites on mesoporous carbons could react with H_2S to successfully convert COS into oxygen. Kan et al.[34] also successfully separated COS by preparing organic carbon-containing basic active sites. Table 3 shows the hydrolysis of COS on different adsorbents.

At present, it is generally believed that the hydrolysis reaction of COS is related to the basic sites on the surface of the catalyst, and hence, the hydrolysis capacity of the catalyst is often improved by increasing the alkalinity of the catalyst, such as increasing the number of nitrogen-containing bases and OH. Fig. 2(a) shows the various types of nitrogen functions observed in NPC materials.[37] The most common types are pyridine nitrogen, pyrrolic nitrogen, and graphitic nitrogen. Other functions include amine, cyano, lactam, triazine, pyridine oxide, and metal coordination nitrogen. Sun et al.[41] studied the reaction process diagram of COS and CS_2 on Cu, as shown in Fig. 2(b) and (c).

After the hydrolysis catalyst reacts, a large amount of sulfur or sulfate will be deposited on the surface of the catalyst, blocking part of the pore size, reducing the specific surface area of the catalyst, and causing the catalyst to be poisoned and deactivated, and the desulfurization conversion rate will decrease. In addition, the reaction process is long, and it is easy to corrode the equipment, which will reduce the quality of the gas. The water vapor and CO_2 generated by the reaction will undergo competitive adsorption with COS, increasing the difficulty of separation, so it is gradually replaced by other means.[43]

1.3 Pyrolysis

Pyrolysis is a method in which COS generates other substances via a thermal decomposition reaction. The reaction mechanism proposed by Partington et al.[44] is now widely accepted. Under anaerobic or anoxic conditions, pyrolysis gases such as CO, H_2 and CH_4 are used to reduce sulfur-containing substances to produce simple sulfur through high temperature.[45] In the

presence of only carbonyl sulfur (COS), the thermal decomposition reaction is as follows:[46]

$$2COS \rightarrow CS_2 + CO_2 \ (CO_2 \ \text{reaction}) \qquad (4)$$

$$COS \rightarrow CO + S \ (CO \ \text{reaction}) \qquad (5)$$
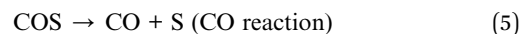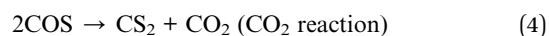
The study shows that the former is under the condition of hot metal platinum, and the latter is catalyzed by silica, in which the reaction of formula (5) is faster than that of formula (4), but the two reaction temperature windows are smaller, and the reverse reaction is very important for desulfurization. The impact of separation is not clear.[46] Moreover, the utilization of pyrolysis method is limited because of low efficiency and high energy consumption.[44]

1.4 Hydrogenation reduction method

The hydrogenation reduction method refers to the method in which COS is converted into H_2S via a hydrogenation reaction and then is removed. The main reaction is shown in formula (6) as follows:[17]

$$COS + H_2 \rightarrow CO + H_2S \qquad (6)$$
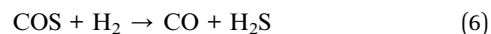
The reaction temperature is medium and high. Commonly used hydrogenation catalysts are binary or multi-element metals such as Co–Mo, Ni–Mo, Ni–W, and Fe–Mn. The main active components are transition metal elements, which are characterized by unfilled d-electron orbitals or hexagonal lattices, and there is a synergistic effect between the two metal elements to promote the hydrogenation reduction reaction. Wang et al.[47] explored the hydro removal effect of Fe–Mn catalysts on COS, pointing out that COS is first converted into H_2S in a reducing atmosphere, and the metal components on the catalyst promote its conversion into metal sulfides and water. Industrial catalysts are mostly prepared by impregnating metal components directly into a γ-Al_2O_3 support. Kamp E. et al.[48] selected Pd/Al_2O_3 to completely convert COS into H_2S at 200 °C, and the results showed that COS dissociated at the Pd site to form CO and S adsorbents, and COS would also adsorb onto the
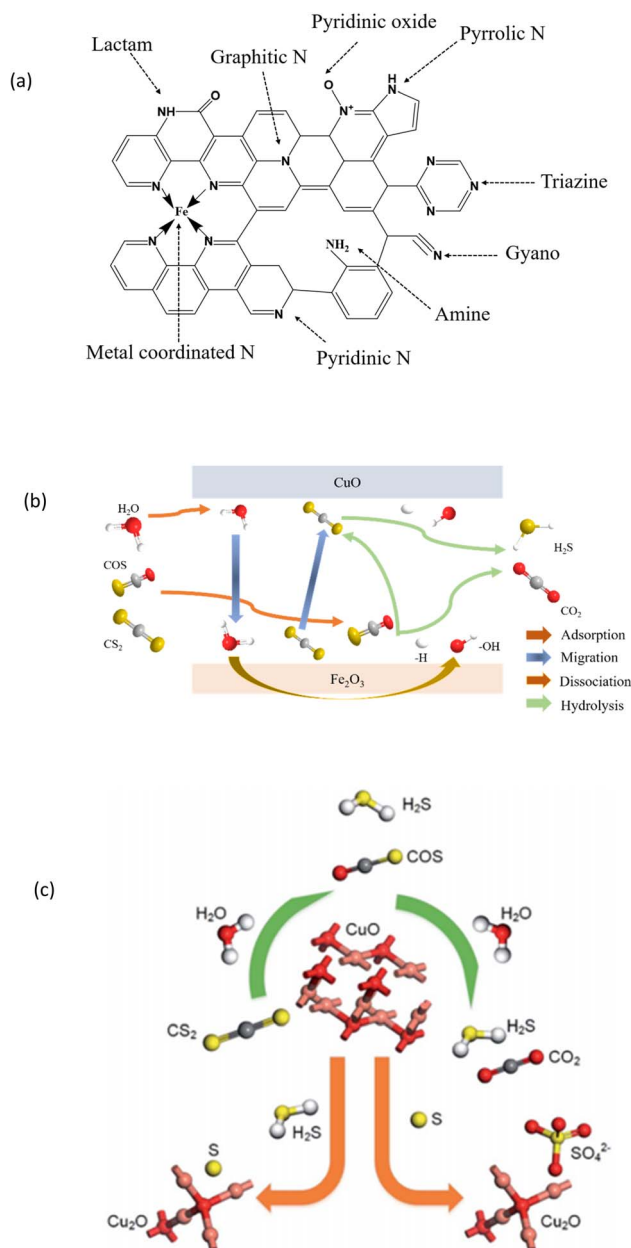
Fig. 2 (a) Different types of nitrogenous sites in NPC (this figure has been adapted/reproduced from ref. 37 with permission from Royal Society of Chemistry, copyright 2016). (b) Hydrolysis mechanism of COS and CS_2 on CuO/Fe_2O_3 catalysts. (c) Reaction process diagram of COS and CS_2 on CuO (this figure has been adapted/reproduced from ref. 41 with permission from Royal Society of Chemistry, copyright 2018).

alumina support, thereby forming $HSCO^{2-}$. Subsequently, $HSCO^{2-}$ reacts with hydroxide surface groups to form carbon dioxide and hydrogen sulfide. In addition, molecular sieves with uniform and tunable mesopores and stable structures are also used as supports for hydrogenation catalysis. It has been studied that Ni–Mo and Co–Mo are supported on the surface of niobium-modified MCM-41, and dibenzothiophene can be separated by hydrogenation.[46]

The hydrogenation reaction can easily separate simple organic sulfur-containing compounds such as thiophene and its derivatives, heterocyclic sulfur compounds,[49] but for the less polar COS, the reaction generates a new pollutant, H_2S,[50] which leads to equipment corrosion,[51,52] increasing the running cost. At the same time, the hydrogenation method requires high reaction temperatures (temperature $\geq$ 400 °C, pressure $\geq$ 10 MPa), the use of hydrogen and precious metals, *etc.*, which require high equipment and control processes. Therefore, this method aims to achieve high removal rates under medium- and low-temperature conditions with low-cost catalysts.

1.5 Adsorption method

The adsorption method can separate one or several components simultaneously in gas using porous materials. Adsorption materials are metal oxides, activated carbon, molecular sieves, metal–organic framework (MOFs), layered double hydroxides (LDHs), *etc.*,[12,53–56] which are characterized by stable and uniform framework structures and can be functionally selected according to separation requirements. Researchers often achieve geometric shape selection through the control of the microscopic morphology of materials. At the same time, metals and/or functional groups are used to modify the adsorption active site, change the electronic spatial structure of the microregion, and improve the adsorption selectivity *via* energy matching to meet the thermodynamic (BET three-constant adsorption isotherm) and kinetic requirements of the adsorption process. Zhao *et al.*[57] prepared a series of nickel-containing hydrotalcite-derived oxides (HTOs) for the removal of COS by co-precipitation and found that Ni_3Al–HTO had the best adsorption effect on COS. The study carried out ion exchange modification on NaX molecular sieves, and through DFT studies, it was concluded that COS achieved separation by forming S–M bonds with metal ions.[55] The adsorption method has been favored by researchers due to its advantages of "plug and play" flexibility, easy operation and control.[55,58–61] Therefore, the research progress and reaction mechanism of COS adsorbents are systematically described below.

2 Carbonyl sulfide adsorption and separation materials

2.1 Metal oxide adsorbents

Metal oxide adsorbents are mainly divided into iron-based, zinc-based, and aluminum-based oxide adsorbents. Due to the special physical and chemical properties of COS, COS is often converted into relatively unstable H_2S for subsequent removal. Table 4 shows the different metal oxides.

However, the desulfurization effect of single metal oxide adsorbents is not ideal, and hence, the desulfurization performance is often improved by adding unsaturated metal active sites *via* compounding metals. Jae *et al.*[71] added rare earth metal Ce on the MgO support, which increased the sulfur adsorption capacity of the adsorbent by about 50 mg g^{-1} on the original basis. Yang *et al.*[29] investigated the desulfurization performance of SnO_2 doped with rare earth

Table 4 Removal of COS on different metal oxides

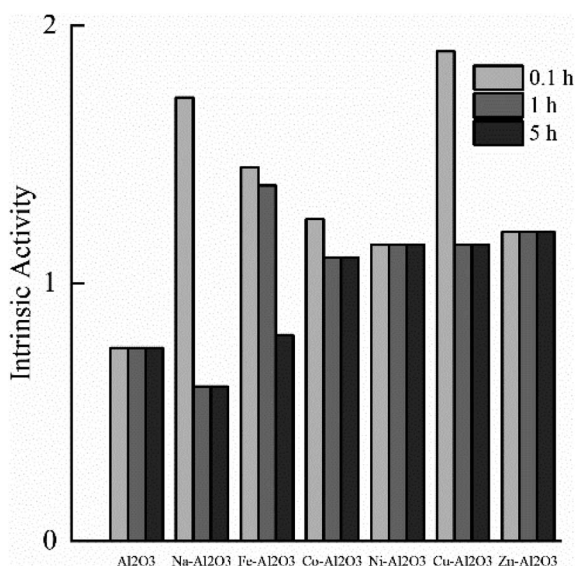| Metal oxide	Reaction formula	The main form	References
Iron base	$Fe_2O_3 \cdot H_2O + 3H_2S \rightarrow Fe_2S_3 \cdot H_2O + 3H_2O$	$\gamma\text{-}Fe_2O_3 \cdot H_2O$ (maghemite)	62–64
	$Fe_2S_3 \cdot H_2O + 3H_2S \rightarrow 2FeS + S + 4H_2O$	$\alpha\text{-}Fe_2O_3 \cdot H_2O$ (haematite)	
Zinc based	$ZnO + COS \rightarrow ZnS + CO_2$	ZnO	65 and 66
	$ZnO + H_2S \rightarrow ZnS + H_2O$		
Manganese base	$COS + H_2 \rightarrow H_2S + CO$	MnO	67
	$COS + H_2O \rightarrow H_2S + CO_2$		
	$MnO + H_2S \rightarrow MnS + H_2O$		
Other	$CuO + H_2S \rightarrow CuS + H_2O$	CuO	68–70

Fig. 3 Reactivity (10^{-6} mol COS hydrolysis per m^2 per h) as a result of reaction time (this figure has been adapted/reproduced from ref. 8 with permission from Elsevier, copyright 2012).

metal La. By comparing the saturated adsorption capacity of different La contents, it was found that with the increase in La loading, the pore size of the adsorbent became larger and the total pore volume increased. When the La content reaches 40%, the adsorbent can provide more catalytically active sites for contacting with COS, thereby improving the

conversion rate of COS. Further research found that metal oxides such as iron-based and zinc-based cannot satisfy both high sulfur capacity and hydrothermal stability.[72,73] In contrast, Al_2O_3 has good hydrothermal stability, and its excellent specific surface area can make active sites disperse uniformly, form a center-radical pore structure, reduce the diffusion resistance of the reaction, and improve the adsorption performance. As shown in Fig. 3, Rupp *et al.*[8] improved the interaction between the catalyst and COS by supporting metal Pd on the $\gamma\text{-}Al_2O_3$ support. In order to improve the hydrolysis ability of COS at low temperatures, by loading transition metals (3 wt% Na, Fe, Co, Ni, Cu, Zn) on γ-Al_2O_3,[74] it was found that the hydrolysis performance of the catalyst except for metallic Na doping was improved, indicating that metal modification could improve the initial and final activities of the hydrolysis reaction.

Both the hydrolysis and hydrogenation reduction reactions involving metal oxides produce H_2S. With the progress of the reaction, the gas diffusion resistance to the solid surface increases, which increases the difficulty of desulfurization and reduces the desulfurization performance. Therefore, ensuring the activity of metal oxides, reducing the occurrence of side reactions, and improving the accessibility of reactions are the focus of later research.

2.2 Activated carbon

Activated carbon is an important adsorption material with abundant microporous structures[75] and many functional
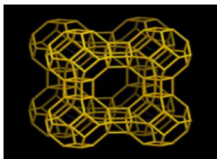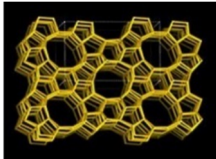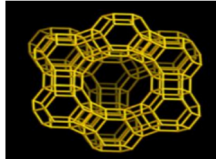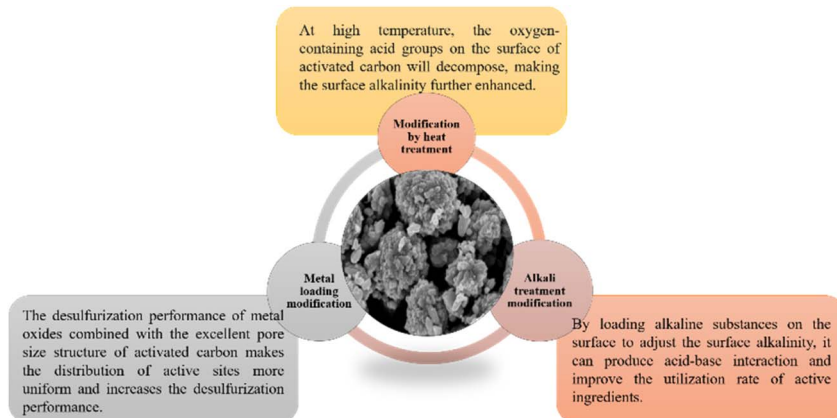

Fig. 4 Different modification methods of activated carbon.

Table 5 Characteristic structures of different molecular sieves

Molecular sieve type	LTA	MFI	FAU
Single cell chemical equation	$Na_{96}Al_{96} \cdot Si_{96} \cdot O_{384} \cdot 216H_2O$	$Na_xAl_x \cdot Si_{96-x} \cdot O_{192} \cdot 16H_2O$	$Na_{86} \cdot Si_{106}Al_{86}O_{384} \cdot 264H_2O$ (Si/Al = 1.23)
Pore structure	Eight-membered ring	Two ten-membered ring cross structure	Twelve-membered ring
Maximum aperture	0.45 nm	0.63 nm	0.8–1.0 nm
Typical representative	Type A molecular sieve	ZSM-5 molecular sieve	X- and Y-type molecular sieves
Schematic			

groups on the surface. Its adsorption capacity can be increased *via* heat treatment modification, alkali treatment modification, and metal loading modification,[33] as shown in Fig. 4. The activated carbon was modified with potassium salts, and the analysis found that potassium ions can be uniformly distributed on the activated carbon, which can improve the saturated sulfur capacity of the adsorbent.[75] The Cu–Co–KW obtained by modifying the KOH-impregnated activated carbon with copper nitrate and sulfonated titanium cyan cobalt (CoPcs) has a saturated sulfur capacity as high as 43.30 mg COS per g. The improvement of adsorption performance is attributed to the combined effect of chemical adsorption and catalytic oxidation, among which chemical adsorption is the main one; in the reaction, an appropriate amount of water hydrolyzes part of COS, impregnation with KOH increases the basic functional groups on the surface of activated carbon, and the doped metal ions can accelerate the catalytic oxidation reaction with COS.[76,77] Melanie *et al.*[78] used activated carbon to adsorb COS and found that adding an appropriate amount of ammonia to the reaction mixture had a positive effect on the adsorption effect. However, activated carbon is mainly composed of micropores (about 95% or more), which play the role of selective adsorption, and its structure is easily collapsable and regeneration is difficult. In the process of industrial application, special attention should be paid to the activation temperature to avoid the effect of activated carbon aching on the desulfurization performance.

2.3 Molecular sieves

A molecular sieve is a general term for a class of crystalline aluminosilicate porous materials with a uniform pore size distribution and selective adsorption effect. Compared with the microporous structural characteristics of activated carbon, different pore sizes and cavities can be formed by connecting oxygen bridges to selectively prepare molecular sieves.[79–81] Some studies have pointed out that the micropores in the molecular sieve provide the active sites for adsorption, and the mesopores increase the diffusion rate of the reaction.[82]

In addition to preparing molecular sieves with different pore sizes, the adsorption effect of molecular sieves can also be improved by surface modification. The cations on the molecular sieve framework can be replaced with other metal ions, to adjust the pore size, surface activity and other properties of the molecular sieve, and further improve the adsorption capacity and selectivity of the molecular sieve. The ion exchange adsorption of thiophene was carried out with metal Cu and Y molecular sieves. It was found that the adsorption capacity of the adsorbent was the best by self-reduction of Cu(II)–Y to Cu(I)–Y. The adsorption form on the adsorbent was assumed, and it was concluded that the adsorption of thiophene was achieved by reacting with proton sites formed by reducing copper on Cu(I)–Y.[83] At 40 °C, the breakthrough adsorption capacity of Ag/NaZSM-5 adsorbent for COS can reach 12.86 mg COS per g, and it shows good regeneration performance when dry air is used as the regeneration purge gas. The adsorption capacity is basically unchanged.[84] Ryzhikov *et al.*[85] selected different metal ions to modify the molecular sieve and found that the adsorption capacity of COS was in the following order: CaX ≈ BaX > NaX > CsNaX > NiNaX > NaY > CsY ≈ NiY. As shown in Table 5, the molecular sieves currently available for desulfurization mainly include: LTA-type molecular sieve, MFI-type molecular sieve and FAU-type molecular sieve.

2.4 Metal–organic frameworks (MOFs)

MOFs are metal–organic framework materials composed of transition metal and organic ligand units self-assembled through coordination bonds. MOF materials have the same controllability of morphology, structure, and crystal size as molecular sieves, and the specific surface area of MOF materials is much larger than that of molecular sieves.[86–89] They have become a popular adsorbent material in recent years. Britt *et al.*[86] used a one-pot method to prepare metal–organic frameworks with different organic ligands, but some metal–organic frameworks have low hydrothermal stability and will compete with water during the adsorption process, resulting in the collapse of the adsorbent structure. The saturated adsorption capacity will decrease. Guo *et al.*[56] synthesized MIL-53(Fe) by hydrothermal synthesis to hydrolyse COS and CS_2, and found that the separation rate of COS was as high as 92.64%, and the 100% separation rate of CS_2 could be maintained for about 30 min. By comparing the adsorption of SO_2 on MOF-74 under different reaction conditions, it was found that the

adsorption rate could reach 100% under dry conditions, but under wet conditions, the adsorption effect was reduced due to the competitive adsorption of water.[90] However, due to the weak polarity of COS, it is still difficult to apply MOFs for separation, which is also the focus of further in-depth research.

2.5 Layered double hydroxides (LDHs)

Layered double hydroxides (LDHs), also known as hydrotalcite (HT) and hydrotalcite-like compounds (HTLCs), are a family of stacked compounds typically made of non-covalent inter layer anions and layer cations. Bond formation, the particle size and distribution of LDHs can be controlled by selectively regulating the types of anions and cations.[16] The layered double metal hydroxide is weakly basic, but the double metal composite oxide (LDO) formed after calcination shows strong basicity and high specific surface area,[91] and has abundant pore size and excellent catalytic performance and is widely used. The adsorption of COS on LDHs-derivative Ni/Mg/Al mixed oxide was 2.47 wt%, and the adsorption rate was almost unchanged after regeneration.[53] The MA-LDHs-3 (Mg/Al = 3) adsorbent prepared by mechanical mixing has a large specific surface area and abundant OH-active sites. At the reaction temperature of 70 °C, the removal rate of COS reaches 100%, but the adsorbent will lose interlayer water at high temperatures, resulting in dehydration of hydroxyl groups on the laminate, resulting in skeleton collapse.[58] Zhao et al.[92] modified the hydrotalcite-derived oxide (HTO) with KOH, which not only increased the basicity of the adsorbent surface but also improved the Lewis basicity of Ni, making the adsorption and removal of COS the best. Although hydrotalcite is rich in basic sites, its specific surface area is small compared to other materials, and it is susceptible to structural collapse due to temperature effects, so the use of LDHs for desulfurization is not widely used.

3 Mechanisms of carbonyl sulfide (COS) separation by adsorption

COS adsorption is the process of being captured and enriched in the surface of the adsorbent, and there are physical and chemical processes, as well as the synergistic effect of the two processes. According to different adsorbents and adsorption reaction conditions, there are different COS adsorption reaction mechanisms.

3.1 Physical adsorption

Physical adsorption is based on intermolecular forces (such as dispersion force, van der Waals force, and hydrogen bonding) to adsorb an adsorbate in the pores or surfaces of materials. Physical adsorption has almost no selectivity, and the adsorption is reversible. COS mainly occurs inside the micropores of the adsorbent, which requires the adsorbent to have a high adsorption capacity and strong selectivity. The Langmuir model is a classic model of physical adsorption that assumes that only a monolayer is formed on the molecular surface, as shown in Fig. 5(a). During the adsorption process, the gas molecules are in an equilibrium state of adsorption and desorption. But in the
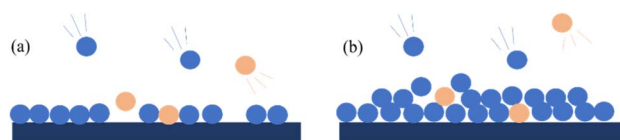

Fig. 5 Simulated distribution of adsorbed gas on adsorbent surface. ((a) Shows simulated monolayer adsorption; (b) shows the multilayer adsorption results).

actual adsorption process, the surface of the adsorbent is not smooth and there is a complex pore structure. Based on the BET theory, it is believed that the physical adsorption of solid to gas is the result of van der Waals gravity, and there is also van der Waals force between molecules, so the adsorbent molecule may be adsorbed when it bumps into the adsorbed molecule, that is to say, the adsorption can form multi-molecular layers, and then multilayer adsorption and accumulation will be carried out on the adsorbent, as shown in Fig. 5(b).

In addition, the physical adsorption process is also controlled by the molecular sieve shape-selective adsorption mechanism. As the molecular sieve has a highly regular pore structure and a specific pore size, it has high selectivity for the size of the adsorbate molecules, but only substances whose molecular dynamics diameter is smaller than its pore size have adsorption capacity. For example, ZSM-5 molecular sieve, although its average pore size is about 0.55 nm, belongs to microporous zeolite, and hence, it can enter and interact with molecular sieves for COS molecules with a kinetic diameter of 0.53 nm. Based on the calculation of the electricity price rule, taking the fukalite molecular sieve as an example, the aluminum–oxygen octahedron $AlO_2(OH)_4$ and the silicon–oxygen tetrahedral structure in the framework make the molecular sieve structure layer display electroneutrality, and the
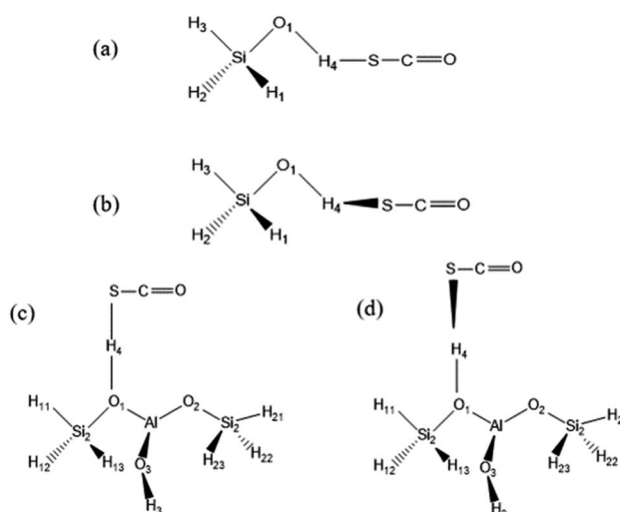

Fig. 6 Four adsorption modes of COS on the silanol and bridging hydroxyl groups ((a) COS is adsorbed in parallel on the silanol; (b) COS is adsorbed vertically on the silanol; (c) COS is adsorbed in parallel on the bridging hydroxyl, and (d) COS is adsorbed vertically on the bridge hydroxyl).

aluminum–oxygen octahedron in the aluminum–oxygen octahedron is electrically neutral. About 60% of the Al–O bonds and Si–O bonds in the silicon–oxygen tetrahedron are ionic bonds and covalent bonds, respectively. Theoretically, the interlayer force of molecular sieves is the combination of hydrogen bonds and van der Waals forces between hydrogen and oxygen atoms.
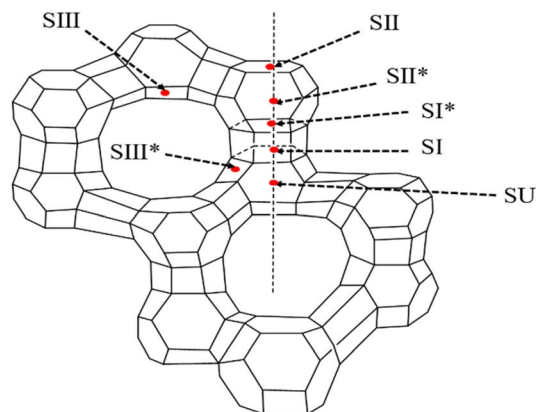

Fig. 7 Cation sites on the FAU-type zeolite framework (this figure has been adapted/reproduced from ref. 95 with permission from American Chemical Society, copyright 1975).
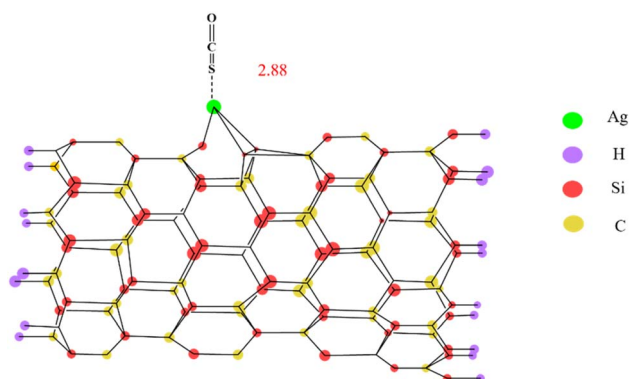

Fig. 8 Stable adsorption model of COS on the Ag–SiCNT adsorbent (this figure has been adapted/reproduced from ref. 99 with permission from Springer, copyright 2015).

Therefore, the adsorption form of COS molecules into the molecular sieve adsorbent is shown in Fig. 6.

3.2 Chemisorption

Complexation, acid–base interaction, and S–M adsorption mechanisms can be divided according to the difference in active centers of COS action. Chemisorption is based on the principle of coordination chemistry, changing the surface acidity and alkalinity of the adsorbent and the distribution of active sites to improve the desulfurization performance.

3.2.1 π-Complexation. Complexation is the formation of complex bonds between the adsorbate and the adsorbent to achieve adsorption and separation. In theory, all transition metal elements in the periodic table, that is, elements in the d block, can produce complex adsorption. When the transition metal atom has a ligand with greater electronegativity (such as F and Cl), due to the large shift of the electron cloud to the ligand, the metal will be partially positively charged, resulting in the outermost layer of the metal. When such metals come into contact with adsorbate molecules (*e.g.* CO and unsaturated hydrocarbons) with π electrons, they are easily receptive to the π electrons provided by the adsorbate to form σ bonds. At the same time, the metal feeds back the excess d electrons of the outer layer to the high-energy antibonding π* orbital of the adsorbed mass space, forming feedback π bonds. The synergistic effect of σ–π bonds enhances the bonding between metals and adsorbate molecules, and π-complex adsorption occurs.[93] Palomino *et al.*[94] used the gas-phase ion exchange (VPIE) method to modify Y molecular sieves, and the resulting Cu(I)–Y(VPIE) molecular sieves had the best terthiophene effect. The metal ion distribution of FAU-type molecular sieves is shown in Fig. 7. Due to the existence of coulombic repulsion, the occupancy of adjacent positions (such as SII and SII*) is rarely studied. It is assumed that the Cu(I)–Y(VPIE) zeolite has a Maxwell cation site distribution,[95] so that Cu$^+$ exposed at the SII and SIII sites is occupied by thiophene molecules, and the remaining Cu$^+$ interacts with other molecules capable of -complexation (aromatic compounds and/or nitrogen heterocycles) for separation purposes.[96]

By analyzing the adsorption effect of Cu–Y on thiophene, it is concluded that some electrons on the p orbital of thiophene are
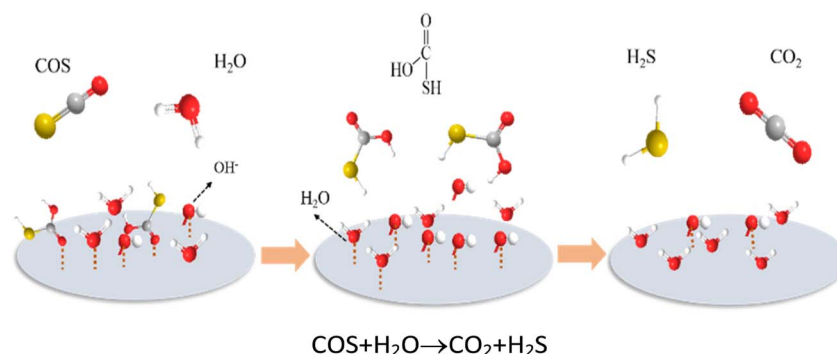

COS+H$_2$O→CO$_2$+H$_2$S

Fig. 9 Schematic diagram of the hydrolysis mechanism of COS on MA-LDHs-*x* (this figure has been adapted/reproduced from ref. 58 with permission from Royal Soceity of Chemistry, copyright 2019).

donated to the empty s orbital of the metal (called an electron donor), and at the same time, the electrons on the d orbital of the metal donate electrons to the p* orbital of thiophene (called a p-donor). Molecular orbital theory further confirms the experimental results.[83] In the case of complexation, the metal ions responsible for the adsorption process provide the transfer of electrons from the highest occupied molecular orbital

(HOMO) to the lowest unoccupied molecular orbital (LUMO). Li et al.[97] discovered that modifying activated carbon with metals such as Cu and Ag increased the amount of COS adsorbed by Cu(I). According to the research, the bond length of Cu(I)–S is shorter than that of Ag(I)–S, indicating that Cu(I)–S has a shorter bond length than that of Ag(I)–S. This is the reason that the -complex bond formed with COS is more stable.
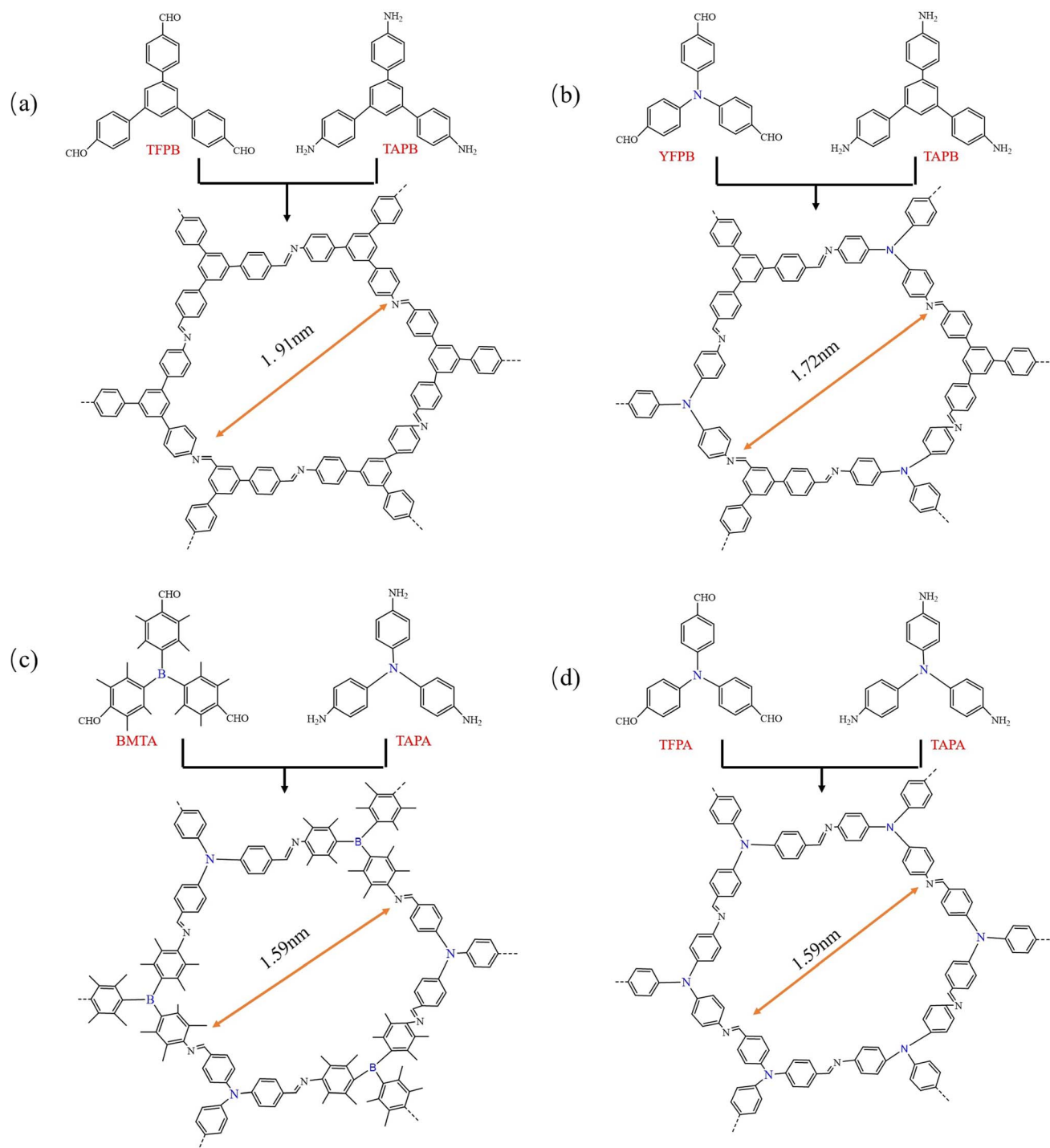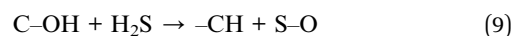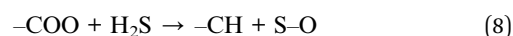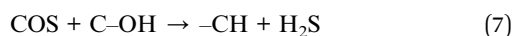

Fig. 10 Synthetic scheme for four imine-linked hexagonal COFs (a–d) varying with the number of triarylamine groups (this figure has been adapted/reproduced from ref. 101 with permission from Royal Soceity of Chemistry, copyright 2017).

3.2.2 Acid–base interaction. The acid–base interaction is achieved by combining the Lewis base sites on the adsorbent surface with the acidic sulfur atoms of organic sulfides to achieve separation. Therefore, in order to increase the Lewis base sites on the surface of the adsorbent, metal salts are commonly used to modify the adsorbent, which are Fe, Cr, Al, *etc.* Song *et al.*[98] combined DRTFIR analysis and found that the more the decrease in C–OH, the more S–O was generated during the catalytic process, so the C–OH group was conducive to the formation of S–O groups, among which –CH, –C–OH, and groups such as –C–OH and –COO play a huge role.

$$COS + C–OH \rightarrow –CH + H_2S \qquad (7)$$

$$–COO + H_2S \rightarrow –CH + S–O \qquad (8)$$

$$C–OH + H_2S \rightarrow –CH + S–O \qquad (9)$$

COS removal process:

$$COS \rightarrow H_2S \rightarrow S \rightarrow SO_4^{2-} \qquad (10)$$

Peyghan *et al.*[99] established the existence of Ag on SiCNT *via* DFT calculations. The analysis showed that the E_{ad} of the combined form in Fig. 8 is the largest (12.20 kcal mol^{-1}). The study found that the hybridization of Ag atoms is close to sp^3, which can provide more electron sites to COS, namely "Lewis's base" to improve the desulfurization performance.

As shown in Fig. 9, Mi *et al.*[58] used MgAl layered double hydroxide (LDH) nanosheets synthesized by a solid mechanochemical method to separate COS. The study pointed out that in the presence of water vapor, COS can pass through ionic dipoles. The sub interaction is adsorbed on the hydroxyl group to form a COS–OH intermediate, which is then reacted with H$_2$O to generate H$_2$S and CO$_2$ for the purpose of separation.

The KOH modified walnut shell biochar catalyst was used to remove COS, and the surface properties of the catalyst were analyzed by the CO$_2$-TPD method.[100] COS and CO$_2$ have similar molecular orbitals and are both Lewis acids, so the adsorption mechanism is similar. As shown in Fig. 10, Zhai *et*

al.[101] compared the adsorption capacity of the number of triaromatic amine groups on CO$_2$ and found that the adsorption capacity of CO$_2$ increased with the increase of the number of triaromatic amine groups, and analyzed that the high adsorption capacity of nitrogenous COFs was due to the existence of nitrogen Lewis bases in the nitrogenous COFs bond and the small pore size. As shown in Fig. 11, Kim *et al.*[75] loaded K onto AC by the impregnation method, and the maximum adsorption capacity was increased to 55.20 mg COS per g. –OH increases the surface alkalinity of the adsorbent and promotes the oxidation of COS, and K$^+$ reacts with –COO to form K$_2$CO$_3$ and COS. At the same time, based on the theory of soft and hard acid–base (HSAB), K$^+$ soft base will more easily combine with S in COS to form K$_2$SCO$_2$, to achieve the purpose of separation.

3.2.3 Sulfur–metal (S–M) direct interaction. The lone pair electrons of the sulfur atom in the organosulfur compound are donated to the metal atom in the adsorbent to directly form the sulfur–metal σ bond.[102–104] At present, the most studied modification method is to add metal oxides to the original adsorbent. Not only can this method increase the content of adsorbed oxygen on the surface of the adsorbent, but introduced metal ions will also form S–M interactions with COS, thereby achieving the purpose of desulfurization.[71,105] The researchers loaded the transition metal onto the Y-type molecular sieve and evaluated its desulfurization performance. The molecular sieve modified with metal Ce was found to have an adsorption capacity of 10 mg g^{-1}. Because Ce ions are f-block elements with high positive charges, the S–M interaction is greater than the formation of -complexes.[106] As shown in Fig. 12, Jiang *et al.*[107] studied the adsorption behavior of COS on the surface of a molecular sieve adsorbent by *in situ* infrared, and found that its adsorption mechanism on the adsorbent surface is mainly divided into two categories. The main adsorption sites in Fig. 12(a) are surface bridge hydroxyl groups (Si–OH–Al) and silyl hydroxyl groups (Si–OH); Fig. 12(b) removes COS on the adsorbent based on the M–S interaction of metal cations with S.

The adsorption process of COS was simulated as shown in Fig. 13. Zhou *et al.*[108] compared the XRD patterns of NiO/ZnO–Al$_2$O$_3$ adsorbents before and after the reaction and found that
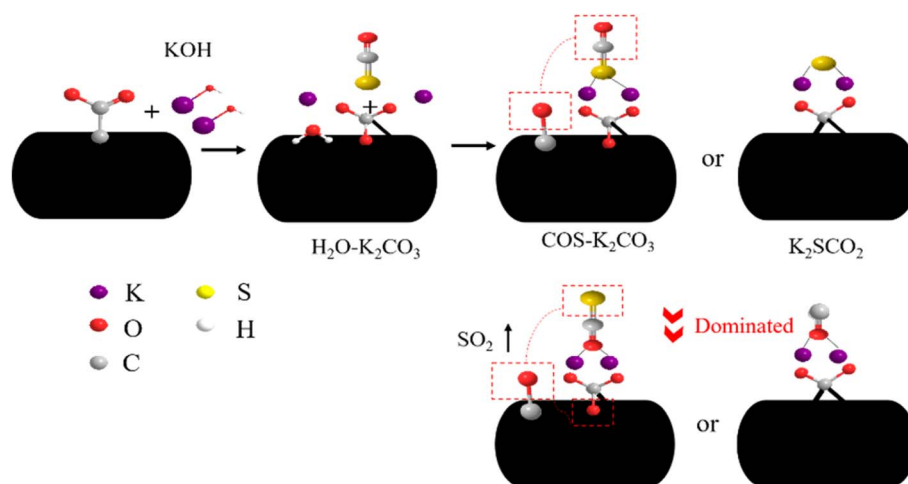

Fig. 11 Diagram of the adsorption mechanism of COS on the surface of AC−K adsorbents.
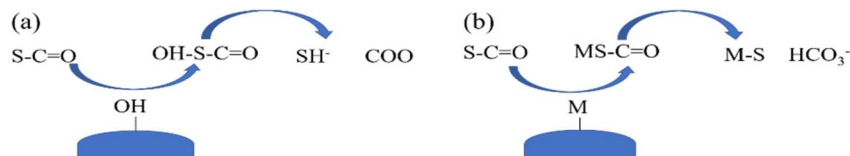
Fig. 12 Two adsorption mechanisms of COS on the surface of adsorbent ((a) to form carbon dioxide and hydrogen sulfide; (b) forming corresponding metal sulfides).
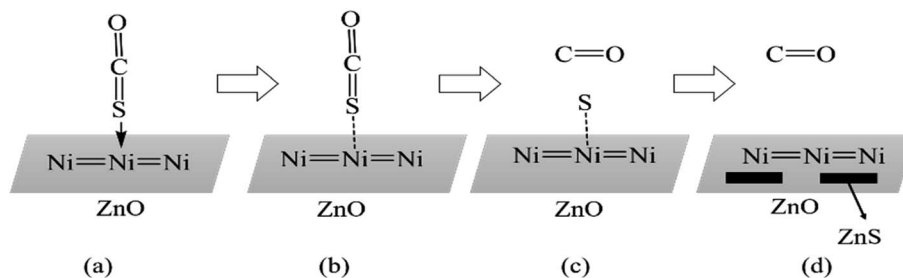

Fig. 13 Desulfurization mechanism of reduced Ni and COS reactions (this figure has been adapted/reproduced from ref. 108 with permission from Elsevier, copyright 2015).

the adsorbent after adsorption showed the characteristic diffraction peaks of ZnS, and the specific surface area and pore volume were significantly reduced, which proved that COS was removed as the form of ZnS, which blocked part of the pore. NiO on the adsorbent surface was reduced to Ni atoms, which combined with S to form an intermediate transition state (Fig. 13(b)). Because the C=S bond is easily broken to form various forms of nickel sulfide, which then reacts with the ZnO carrier to form ZnS, achieving the goal of separation and regeneration *via* high-temperature calcination.

In the case of HKUST-1, the copper atom in the frame is coordinated by the tricarboxylate (BTC) linker and four oxygen of the water molecule to form a face-centered cubic crystal, which contains large square pores (9.9 A), and then a frame of empty Cu^{2+} species is formed *via* a dehydration process. The coordination unsaturated Cu^{2+} cations constitute a surface ion pair, which plays a role in the adsorption process.[109] Song *et al.*[98] supported Fe species on the modified walnut shell biochar catalyst (abbreviation: KOH/WSB) and found that the medium-strength Fe–S binding energy (−4.5 eV) had the best performance. The iron ion shell was an unfilled structure, which gives it more nuclear charge, and this structure facilitates the formation of coordination compounds during the reaction. Coordination compounds, as intermediate products, can provide coordination catalysis and the corresponding surface reactions, thereby promoting catalytic reactions.

4 Conclusion and outlook

Under the background of "ultra-low emissions" in the iron and steel industry, the implementation of BFG's sulfide control can greatly reduce the overall SO_2 emissions. Therefore, BFG desulfurization is imperative. The adsorption method to remove carbonyl sulfide has the advantages of convenient operation, no

by-products, rich adsorbent, *etc.*, and its adsorption mechanism is divided into two types: physical adsorption and chemical adsorption. The former is the use of intermolecular forces to achieve the removal effect, such as the selective catalytic effect of molecular sieves. The latter chemical adsorption is based on the formation of a new bond between the active site on the adsorbent and the carbonyl sulfide, and the old fracture completes the adsorption, such as π complexation, S–M, and σ bonding. In the adsorption process, the solitary pair electrons of sulfur atoms in organic sulfur and the adsorbent containing π electrons combine with the metal atoms in the adsorbent to form sulfur–metal σ bonds and π–σ bonds, so that simple substances S and sulfates are formed on the surface of the adsorbent to achieve the purpose of removal. The core technical difficulty of BFG desulfurization is that the sulfur capacity and selectivity of the adsorbent cannot meet the requirements of industrial applications under complex working conditions. Therefore, industrial adsorbents of BFG desulfurization that can effectively remove a variety of sulfides and have economic competitiveness under the practical working conditions have become the research hotspot. This paper introduces the industrial application of BFG desulfurization and the research progress of COS. Combined with the core requirements of BFG desulfurization, this paper points out the research direction of COS adsorption materials and adsorption separation process in the future.

Conflicts of interest

There are no conflicts to declare.

References

1 K. Jones, *Politics vs. economics in world steel trade*, Routledge, 2017.

2 W. Huang, Z. Qin, Y. L. Qu, *et al.*, Operation Analysis of Steel Industry in 2021 and Outlook in 2022, *Smelting Gold Economics and Management*, 2022, vol. 1, pp. 19–21.

3 J. Qie, C. Zhang, *et al.*, Material flow analysis of zinc during the manufacturing process in integrated steel mills in China, *J. Ind. Ecol.*, 2021, **25**(4), 1009–1020.

4 D. Leeson, J. Fairclough and C. Petit, *et al.*, A systematic review of current technology and cost for industrial carbon capture, Imperial College London, Grantham Institute, Report GR7, 2014.

5 I. Jamil and R. Jamil, Application and Development Trend of Flue Gas Desulfurization (FGD) Process, A Review, *Int. J. Innovation Appl. Stud.*, 2013, **4**(2), 286–297.

6 P. S. Nolan, *Flue gas desulfurization technologies for coal-fired power plants*, The Babcock & Wilcox Company, 2000.

7 Z. Sun, J. Liu and Z. Sun, Synergistic decarbonization and desulfurization of blast furnace gas via a novel magnesium-molybdenum looping process, *Fuel*, 2020, **279**, 118–418.

8 E. C. Rupp, E. J. Granite and D. C. Stanko, Catalytic formation of carbonyl sulfide during warm gas clean-up of simulated coal-derived fuel gas with $Pd/\gamma-Al_2O_3$ sorbents, *Fuel*, 2012, **92**, 211–215.

9 Á. A. Ramirez-santos, C. Castel and E. Favre, A review of gas separation technologies within emission reduction programs in the iron and steel sector, current application and development perspectives, *Sep. Purif. Technol.*, 2018, **194**, 425–442.

10 W. Zhu, X. Peng and Y. Hui, Study on the foaming of MDEA desulfurization solution, *Chem. Eng. Oil Gas*, 2015, **44**(2), 22–27.

11 J. Pang, X. Q. Zhang and X. T. Pang, Use of MSQ-3 desulfurization catalyst in desulfurization of semi-water gas, *Henan Sci.*, 2004, **31**(3), 45–47.

12 N. M. Galea, J. LO and T. Ziealea, A DFT study on the removal of adsorbed sulfur from a nickel (111) surface, Reducing anode poisoning, *J. Catal.*, 2009, **263**, 380–389.

13 M. Asadullah, T. Miyazawa, S. I. Ito, *et al.*, Gasification of different biomasses in a dual-bed gasifier system combined with novel catalysts with high energy efficiency, *Appl. Catal., A*, 2004, **267**, 95–102.

14 Y. Liu, J. Ma and H. He, Heterogeneous reactions of carbonyl sulfide on mineral oxides, mechanism and kinetics study, *Atmos. Chem. Phys.*, 2010, **10**, 10335–10344.

15 P. D. Vaidya and E. Y. Kenig, Kinetics of carbonyl sulfide reaction with alkanolamines, a review, *Chem. Eng. J.*, 2009, **148**, 207–211.

16 R. Farrauto, S. Hwang, L. Shore, *et al.*, New Material Needs for Hydrocarbon Fuel Processing, Generating Hydrogen for the PEM Fuel Cell, *Annu. Rev. Mater. Res.*, 2003, **33**, 1–27.

17 C. Rhodes, S. A. Riddel, J. West, *et al.*, The low-temperature hydrolysis of carbonyl sulfide and carbon disulfide, a review, *Catal. Today*, 2000, **59**(3–4), 443–464.

18 H. X. Guo, M. Q. Miao, Y. Q. Zhang, *et al.*, Review and prospect of desulfurization technology development in China, *Coal Chem. Ind.*, 2003, **31**(2), 51–54.

19 C. T. Molina, R. Riveratinoco and C. Boualluo, Adaptive Random Search Method + Genetic Algorithms for reaction kinetics modelling, CO_2 absorption systems, *Chem. Eng. Trans.*, 2011, **25**, 19–24.

20 F. Amararene and C. Boualluo, Kinetics of Carbonyl Sulfide (COS) Absorption with Aqueous Solutions of Diethanolamine and Methyl diethanolamine, *Ind. Eng. Chem. Res.*, 2004, **43**, 6136–6141.

21 M. M. Sharma, Kinetics of reactions of carbonyl sulphide and carbon dioxide with amines and catalysis by Brønsted bases of the hydrolysis of COS, *Trans. Faraday Soc.*, 1965, **61**, 681–688.

22 R. J. Littel, G. F. Versteeg and W. Swaaij, Kinetics of COS with primary and secondary amines in aqueous solutions, *AIChE J.*, 1992, **38**(2), 244–250.

23 M. Singh and J. A. Bullin, Determination of rate constants for the reaction between diglycolamine and carbonyl sulphide, *Gas Sep. Purif.*, 1988, **2**(3), 131–137.

24 H. A. Al-Ghawas, G. Ruiz-Ibanez and O. C. Sandall, Absorption of carbonyl sulfide in aqueous methyl diethanolamine, *Chem. Eng. Sci.*, 1989, **44**(3), 631–639.

25 R. Rivera-Tinoco and C. Bouallou, Reaction kinetics of carbonyl sulfide (COS) with diethanolamine in methanolic solutions, *Ind. Eng. Chem. Res.*, 2008, **47**(19), 7375–7380.

26 A. Valtz, C. Coqnelet and D. Richon, Volumetric properties of the monoethanolamine–methanol mixture at atmospheric pressure from 283.15 to 353.15K, *Thermochim. Acta*, 2005, **428**, 185–191.

27 M. Ke, D. Chen, Q. Feng, *et al.*, Research on reaction mechanism and kinetics of carbonyl sulfur and alcoholamine solution, *Chem. Sci. Technol.*, 2014, **22**(6), 71–74.

28 N. Tippayawong and P. Thanompongchart, Biogas quality upgrade by simultaneous removal of CO_2 and H_2S in a packed column reactor, *Energy*, 2010, **35**(12), 4531–4535.

29 Y. Yang, Y. Shi and N. Cai, Simultaneous removal of COS and H_2S from hot syngas by rare earth metal-doped SnO_2 sorbents, *Fuel*, 2016, **181**, 1020–1026.

30 Z. Shun, H. Zhao, *et al.*, ChemInform Abstract, The Hydrolysis of Carbonyl Sulfide at Low Temperature, A Review, *ChemInform*, 2014, **45**, 443–464.

31 L. Wang, S. Wang, Q. Yuan, *et al.*, COS hydrolysis in the presence of oxygen, experiment and modeling, *J. Nat. Gas Chem.*, 2008, **17**(1), 93–97.

32 D. Chiche and J. M. Schweitzer, Investigation of competitive COS and HCN hydrolysis reactions upon an industrial catalyst, Langmuir-Hinshelwood kinetics modeling, *Appl. Catal., B*, 2017, **205**, 189–200.

33 S. Liang, J. Mi, F. Liu, *et al.*, Efficient catalytic elimination of COS and H_2S by developing ordered mesoporous carbons with versatile base N sites via a calcination induced self-assembly route, *Chem. Eng. Sci.*, 2020, **221**, 115714.

34 X. Kan, G. Zhang, Y. Luo, *et al.*, Efficient catalytic removal of COS and H2S over graphitized 2D micro-meso-macroporous carbons endowed with ample nitrogen sites synthesized via mechanochemical carbonization, *Green Energy Environ.*, 2022, **7**(5), 983–995.

35 H. Guo, L. Tang, K. Li, *et al.*, Influence of the preparation conditions of MgAlCe catalysts on the catalytic hydrolysis of carbonyl sulfide at low temperature, *RSC Adv.*, 2015, **5**(26), 20530–20537.

36 K. Li, G. Liu, C. Wang, *et al.*, Acidic and basic groups introducing on the surface of activated carbon during the plasma-surface modification for changing of COS catalytic hydrolysis activity, *Catal. Commun.*, 2020, **144**, 106093.

37 M. Li, X. Fan, H. Li, *et al.*, Nitrogen-doped porous carbon materials: promising catalysts or catalyst supports for heterogeneous hydrogenation and oxidation, *Catal. Sci. Technol.*, 2016, **6**(11), 3670–3693.

38 X. Song, X. Chen, L. Sun, *et al.*, Synergistic effect of Fe_2O_3 and CuO on simultaneous catalytic hydrolysis of COS and CS_2, experimental and theoretical studies, *Chem. Eng. J.*, 2020, **399**, 125764.

39 X. Song, L. Sun, H. Guo, *et al.*, Experimental and Theoretical Studies on the Influence of Carrier Gas for COS Catalytic Hydrolysis over MgAlCe Composite Oxides, *ACS Omega*, 2019, **4**(4), 7122–7127.

40 D. Chiche and J. M. Schweitzer, Investigation of competitive COS and HCN hydrolysis reactions upon an industrial catalyst, Langmuir-Hinshelwood kinetics modeling, *Appl. Catal., B*, 2017, **205**, 189–200.

41 S. Xin, H. Ruan, S. Xin, *et al.*, Research into the reaction process and the effect of reaction conditions on the simultaneous removal of H_2S, COS and CS_2 at low temperature, *RSC Adv.*, 2018, **8**(13), 6996–7004.

42 N. Ping, S. Xin, L. Kai, *et al.*, Catalytic hydrolysis of carbonyl sulphide and carbon disulphide over Fe_2O_3 cluster: Competitive adsorption and reaction mechanism, *Sci. Rep.*, 2017, **7**(1), 14452.

43 X. Zhang, Y. Tang, S. Qu, *et al.*, H_2S-selective catalytic oxidation, catalysts and processes, *ACS Catal.*, 2015, **5**(2), 1053–1067.

44 J. R. Partington and H. H. Neville, The thermal decomposition of carbonyl sulphide, *J. Chem. Soc.*, 1951, 1230.

45 G. N. Lewis and W. N. Lacey, The equilibrium between carbon oxysulfide, carbon monoxide and sulfur, *J. Am. Chem. Soc.*, 1915, **37**(9), 1976–1983.

46 F. J. Méndez, O. E. Franco-López, X. Bokhimi, *et al.*, Dibenzothiophene hydrodesulfurization with NiMo and CoMo catalysts supported on niobium-modified MCM-41, *Appl. Catal., B*, 2017, **219**, 479–491.

47 F. F. Wang, H. Zhao, D. X. Zhang, *et al.*, The mechanism of desulfurization of carbonyl sulfur in coal gas by Fe – Mn desulfurizer Exploration, *J. China Coal Soc.*, 2008, **33**(2), 197–200.

48 E. Kamp, H. Thielert, O. von Morstein, *et al.*, Investigation on the simultaneous removal of COS, CS_2 and O_2 from coke oven gas by hydrogenation on a Pd/Al_2O_3 catalyst, *Catal. Sci. Technol.*, 2020, **10**(9), 2961–2969.

49 D. T. Tran, J. M. Palomino and S. R. J. Oliver, Desulfurization of JP-8 jet fuel, challenges and adsorptive materials, *RSC Adv.*, 2018, **8**(13), 7301–7314.

50 K. O. Blumberg, M. P. Walsh and C. Pera, *Low-Sulfur Gasoline & Diesel, The Key To Lower Vehicle Emissions*, 2003.

51 B. Saha, S. Vedachalam and A. K. Dalai, Review on recent advances in adsorptive desulfurization, *Fuel Process. Technol.*, 2021, **214**, 106685.

52 X. Wang, L. Ding, Z. Zhao, *et al.*, Novel hydrodesulfurization nano-catalysts derived from Co_3O_4 nanocrystals with different shapes, *Catal. Today*, 2011, **175**(1), 509–514.

53 D. E. Sparks, T. Morgan, P. M. Patterson, *et al.*, New sulfur adsorbents derived from layered double hydroxides, I, synthesis and COS adsorption, *Appl. Catal., B*, 2008, **82**(3–4), 190–198.

54 K. Sakanishi, Z. Wu, A. Matsumura, *et al.*, Simultaneous removal of H_2S and COS using activated carbons and their supported catalysts, *Catal. Today*, 2005, **104**(1), 94–100.

55 X. Chen, B. Shen and H. Sun, Ion-exchange modified zeolites X for selective adsorption desulfurization from Claus tail gas, experimental and computational investigations, *Microporous Mesoporous Mater.*, 2018, **261**, 227–236.

56 Q. X. Guo, K. Li, Y. X. Ma, *et al.*, Low temperature removal of COS and CS_2 from metal organic framework material MIL-53(Fe), *Mod. Chem. Ind.*, 2020, **40**(S1), 107–110.

57 S. Zhao, H. Yi, X. Tang, *et al.*, Mechanism of activity enhancement of the Ni based hydrotalcite-derived materials in carbonyl sulfide removal, *Mater. Chem. Phys.*, 2018, **205**, 35–43.

58 J. Mi, X. Chen, Q. Zhang, *et al.*, Mechanochemically synthesized MgAl layered double hydroxide nanosheets for efficient catalytic removal of carbonyl sulfide and H_2S, *Chem. Commun.*, 2019, **55**(63), 9375–9378.

59 F. Adib, A. Bagreev and T. J. Bandosz, Analysis of the relationship between H_2S removal capacity and surface properties of unimpregnated activated carbons, *Environ. Sci. Technol.*, 2000, **34**(4), 686–692.

60 Y. H. Kong, G. X. Wang, X. H. Wang, *et al.*, New progress and application of temperature fine desulfurization process, *Nitrogen Fertilizer Design*, 1995, vol. 33(3), pp. 50–54.

61 L. Lv, J. Zhang, C. Huang, *et al.*, Adsorptive separation of dimethyl disulfide from liquefied petroleum gas by different zeolites and selectivity study via FT-IR, *Sep. Purif. Technol.*, 2014, **125**, 247–255.

62 Y. Yang and S. T. Tong, Research progress of iron oxide desulfurizer at room temperature, *Gas Heat*, 2002, **22**(4), 3.

63 G. Huang, E. He, *et al.*, Synthesis and Characterization of γ-Fe2O3 for H2S Removal at Low Temperature, *Ind. Eng. Chem. Res.*, 2015, **54**(34), 8469–8478.

64 H. L. Fan, T. Sun, Y. P. Zhao, *et al.*, Three-Dimensionally Ordered Macroporous Iron Oxide for Removal of H_2S at Medium Temperatures, *Environ. Sci. Technol.*, 2013, **47**(9), 4859–4865.

65 M. X. Tang, X. K. Li, Z. J. Lv, *et al.*, Study on removal of sulfur from benzene by hydrosorption over Ni/ZnO catalyst, *J. Fuel Chem. Technol.*, 2009, **37**(6), 6.

66 C. Yang, J. Wang, H. L. Fan, *et al.*, Contributions of tailored oxygen vacancies in ZnO/Al$_2$O$_3$ composites to the enhanced ability for H$_2$S removal at room temperature, *Fuel*, 2018, **215**(Mar. 1), 695–703.

67 T. Kyotani, H. Kawashima, A. Tomita, *et al.*, Preparation of Nano-sized manganese oxide desulfurization agent for flue gas, *Tangshan Normal University Acta Petrolei Sinica*, 2007, **29**(5), 3.

68 T. Kyotani, H. Kawashima, A. Tomita, *et al.*, Removal of H$_2$S from hot gas in the presence of Cu-containing sorbents, *Fuel*, 1989, **68**(1), 74–79.

69 J. W. Guo, *Preparation of Cu–Zn adsorbent and its mechanism of thiophene removal from coke oven gas*, Taiyuan University of Technology, 2020.

70 D. Liu, S. Chen, X. Fei, *et al.*, Regenerable CuO-Based Adsorbents for Low Temperature Desulfurization Application, *Ind. Eng. Chem. Res.*, 2015, **54**(14), 3556–3562.

71 L. S. Jae, H. K. Jun, S. Y. Jung, *et al.*, Regenerable MgO-based SOx removal sorbents promoted with cerium and iron oxide in RFCC, *Ind. Eng. Chem. Res.*, 2005, **44**(26), 9973–9978.

72 H. Fan, C. Li and K. Xie, Sorbents for high-temperature removal of hydrogen sulfide from coal-derived fuel gas, *J. Nat. Gas Chem.*, 2001, **10**(3), 256–270.

73 C. Du, The use of organic sulfur hydroconversion catalysts, *Ind. Catal.*, 2003, **11**(9), 13.

74 J. West, B. P. Williams, N. Young, *et al.*, Ni-and Zn-promotion of γ-Al$_2$O$_3$ for the hydrolysis of COS under mild conditions, *Catal. Commun.*, 2001, **2**(3–4), 135–138.

75 J. Kim, J. Y. Do, K. Nahm, *et al.*, Capturing ability for COS gas by a strong bridge bonding of a pair of potassium anchored on carbonate of activated carbon at low temperatures, *Sep. Purif. Technol.*, 2019, **211**, 421–429.

76 J. Qiu, P. Ning, X. Wang, *et al.*, Removing carbonyl sulfide with metal-modified activated carbon, *Front. Environ. Sci. Eng.*, 2016, **10**(1), 11–18.

77 X. Wang, J. Qiu, N. Ping, *et al.*, Adsorption/desorption of low concentration of carbonyl sulfide by impregnated activated carbon under micro-oxygen conditions, *J. Hazard. Mater.*, 2012, 128–136.

78 M. L. Sattler and R. S. Rosenberk, Removal of Carbonyl Sulfide Using Activated Carbon Adsorption, *J. Air Waste Manage. Assoc.*, 2006, **56**, 219–224.

79 M. E. Davis and R. F. Lobo, Zeolite and molecular sieve synthesis, *Chem. Mater.*, 1992, **4**(4), 756–768.

80 C. W. Jones, K. Tsuji and M. E. Davis, Organic-functionalized molecular sieves as shape-selective catalysts, *Nature*, 1998, **393**, 52–54.

81 S. M. Csicsery, Shape-selective catalysis in zeolites, *Zeolites*, 1984, (4), 202–213.

82 S. Y. Yuan, *Preparation and desulfurization performance of metal-doped ZSM-5 molecular sieve*, Henan University, 2018.

83 R. T. Yang, A. Takaha and F. H. Yang, New sorbents for desulfurization of liquid fuels by π-complexation, *Ind. Eng. Chem. Res.*, 2001, **40**(26), 6236–6239.

84 Y. Wang, S. Chen, H. Chen, *et al.*, Removal of carbonyl sulfide from CO$_2$ stream using AgNO$_3$ -modified NaZSM-5, *J. Energy Chem.*, 2013, **22**(6), 902–906.

85 A. Ryzhikov, V. Hulea, D. Tichit, *et al.*, Methyl mercaptan and carbonyl sulfide traces removal through adsorption and catalysis on zeolites and layered double hydroxides, *Appl. Catal., A*, 2011, **397**(1–2), 218–224.

86 D. Britt, D. Tranchemontagne and O. M. Yaghi, Metal-organic frameworks with high capacity and selectivity for harmful gases, *Proc. Natl. Acad. Sci. U. S. A.*, 2008, **105**, 11623–11627.

87 O. M. Yaghi, M. O'keeffe, N. W. Ockwig, *et al.*, Reticular synthesis and the design of new materials, *Nature*, 2003, **423**, 705–714.

88 S. Kitagawa, Metal–organic frameworks (MOFs), *Chem. Soc. Rev.*, 2014, **43**(16), 5415–5418.

89 P. Brandt, A. Nuhnen, M. Lange, *et al.*, Metal–organic frameworks with potential application for SO$_2$ separation and flue gas desulfurization, *ACS Appl. Mater. Interfaces*, 2019, **11**(19), 17350–17358.

90 T. G. Glover, G. W. Peterson, B. J. Schindler, *et al.*, MOF-74 building unit has a direct impact on toxic gas adsorption, *Chem. Eng. Sci.*, 2011, **66**, 163–170.

91 M. R Ciulete, G. Layrac, F. Papa, *et al.*, Influence of Mn content on the catalytic properties of Cu-(Mn)-Zn-Mg-Al mixed oxides derived from LDH precursors in the total oxidation of methane, *Catal. Today*, 2018, **306**, 276–286.

92 S. Zhao, X. Tang, M. He, *et al.*, The potential mechanism of potassium promoting effect in the removal of COS over K/NiAlO mixed oxides, *Sep. Purif. Technol.*, 2017, **194**, 33–39.

93 Y. M. Zhou, X. Q. Liu and H. Q. Yao, Research progress of π complex adsorption separation technology, *Petrochem. Ind.*, 2005, **34**(10), 1004–1009.

94 G. T. Palomino, S. Bordiga, A. Zecchina, *et al.*, XRD, XAS, and IR characterization of copper-exchanged Y zeolite, The, *J. Phys. Chem. B*, 2000, **104**, 8641–8651.

95 I. Maxwell and J. De Boer, Crystal structures and dehydrated divalent-copper-exchanged faujasite, *J. Phys. Chem.*, 1975, **79**, 1874–1879.

96 A. Hernández-Maldonado, F. H. Yang, G. Qi, *et al.*, Desulfurization of transportation fuels by π-complexation sorbents, Cu(I)-, Ni(II)-, and Zn(II)-zeolites, *Appl. Catal., B*, 2005, **56**, 111–126.

97 M. Li, Z. H. Zhang and Y. Wei, Removal of low concentration carbonyl sulfur from activated carbon modified by Cu and Ag at room temperature, *Fine Chemical Industry*, 2016, **33**(4), 6.

98 X. Song, P. Ning, C. Wang, *et al.*, Research on the low temperature catalytic hydrolysis of COS and CS$_2$ over walnut shell biochar modified by Fe–Cu mixed metal oxides and basic functional groups, *Chem. Eng. J.*, 2016, **314**(Complete), 418–433.

99 A. A. Peyghan, H. Soleymanabadi and Z. Bagheri, Theoretical study of carbonyl sulfide adsorption on Ag-doped SiC nanotubes, *J. Iran. Chem. Soc.*, 2015, **12**, 1071–1076.

100 X. Song, K. Li, C. Wang, *et al.*, Regeneration performance and mechanism of modified walnut shell biochar catalyst for low temperature catalytic hydrolysis of organic sulfur, *Chem. Eng. J.*, 2017, **330**, 727–735.

101 L. Zhai, N. Huang, H. Xu, *et al.*, A backbone design principle for covalent organic frameworks: the impact of weakly interacting units on CO_2 adsorption, *Chem. Commun.*, 2017, **53**(30), 4242–4245.

102 R. Dehghan and M. Anbia, Zeolites for adsorptive desulfurization from fuels, a review, *Fuel Process. Technol.*, 2017, **167**, 99–116.

103 G. I. Danmaliki, T. A. Saleh and A. A. Shamsuddeen, Response surface methodology optimization of adsorptive desulfurization on nickel/activated carbon, *Chem. Eng. J.*, 2017, **313**, 993–1003.

104 B. Yoosuk, A. Silajan and P. Prasassarakich, Deep adsorptive desulfurization over ion-exchanged zeolites: Individual and simultaneous effect of aromatic and nitrogen compounds, *J. Clean. Prod.*, 2020, **248**, 119291.

105 H. L. Sun, Y. Liu and S. W. Liu, Study on Manganese-Cerium Mixed Oxide Aerogel Catalysts, *J. Fuel Chem. Technol.*, 2004, **32**(1), 93–97.

106 S. Velu, X. Ma and C. Song, Zeolite-based adsorbents for desulfurization of jet fuel by selective adsorption, *Am. Chem. Soc.*, 2002, **47**(2), 447–448.

107 H. M. Jiang, *Adsorption and mechanism of carbonyl sulfur and hydrogen sulfide from coke oven gas by molecular sieve*, Taiyuan University of Technology, 2021.

108 G. L. Zhou, M. Q. Wang, X. S. Wang, *et al.*, Adsorption removal of COS from coke oven gas by NiO/ZnO-Al_2O_3 adsorbent, *J. Fuel Chem. Technol.*, 2015, (4), 470–475.

109 K. Vellingiri, A. Deep and K. H. Kim, Metal–organic frameworks as a potential platform for selective treatment of gaseous sulfur compounds, *ACS Appl. Mater. Interfaces*, 2016, **8**(44), 29835–29857.